Electronic Supplementary Material (ESI) for Analyst.

Microfluidic device for multiplexed detection of fungal infection biomarkers in grape cultivars

Eduardo J.S.Brás[1,2], Ana Margarida Fortes[3], Teresa Esteves[2,4] Virginia Chu[1], Pedro Fernandes[2,5], João Pedro Conde[1,4*]

[1] Instituto de Engenharia de Sistemas e Computadores – Microsistemas e Nanotecnologias (INESC MN)
[2] IBB – Institute for Bioengineering and Biosciences, Instituto Superior Técnico, Universidade de Lisboa, Lisbon, Portugal
[3]BioISI, Faculdade de Ciências de Lisboa, Universidade de Lisboa , Lisbon, Portugal
[4] Department of Bioengineering, Instituto Superior Técnico, Universidade de Lisboa, Lisbon, Portugal
[5] DREAMS and Faculty of Engineering, Universidade Lusófona de Humanidades e Tecnologias, Lisbon, Portugal
***** Corresponding author: joao.conde@tecnico.ulisboa.pt

S1 – Jasmonic acid – BSA conjugation

In this work, a conjugation between jasmonic acid (JA) and bovine serum albumin (BSA) is performed in order to immobilize JA on the microbead surface. To confirm the conjugation of JA to the BSA molecules, both were incubated at 5 g/L with the silica microbeads for 1h under constant agitation. Then, both functionalized beads were packed into a micro-column and the labelled α-JA antibody was injected for 5 min at a concentration of 50 mg/L at a flow rate of 1 µL/min, followed by a 1 min washing step with PBS at 5 µL/min. The results obtained are presented in Figure S1.

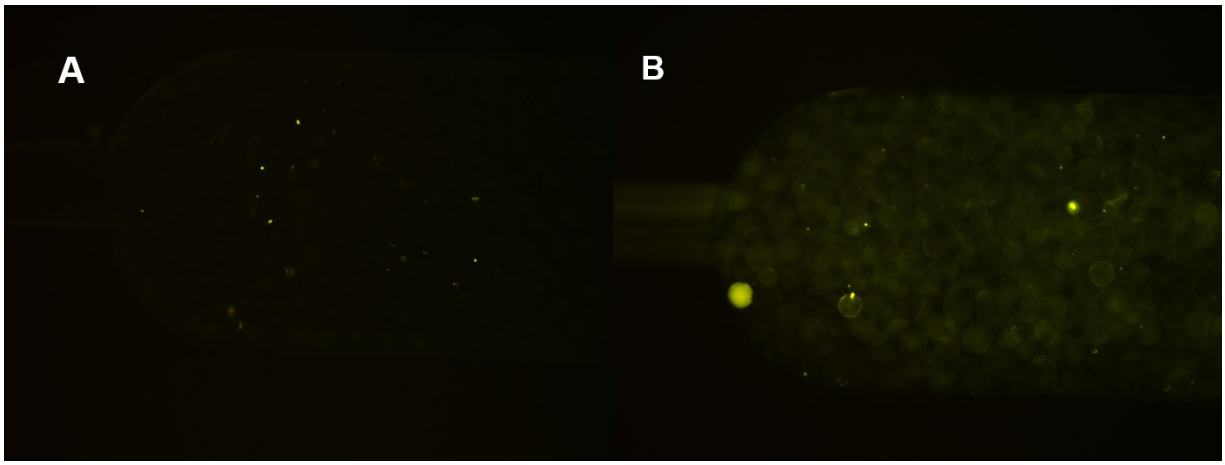

Figure S1 – Results obtained concerning the interaction between the α-JA antibody with microbeads functionalized with BSA (A) and JA-BSA (B). Pictures were enhanced for visualization purposes.

The results presented demonstrate that the antibody does not interact with the BSA functionalized beads, however it does attach to the JA-BSA beads. These results also motivated the use of BSA as the blocking agent of the assay.

S1 – Photosensor Characterization

In this work, a thin-film amorphous silicon photosensor array is used as an optical transducer for the different detection methods used. The active layer of the sensor is a 200 µm x 200 µm and is composed of a 500 nm thick layer of intrinsic hydrogenated amorphous silicon. The deposition conditions for the film using an Oxford Plasma Pro 100 were: Temperature= 300 ˚C, Chamber Pressure= 350 mTorr, RF Power= 10 W, SiH_4 flow rate= 25 sccm, H_2 flow rate= 10 sccm, Deposition time= 21 min. The *I-V* curve as well as

the photoresponse of the sensors at the wavelengths of interest for the absorbance assays are shown in Figure S2.

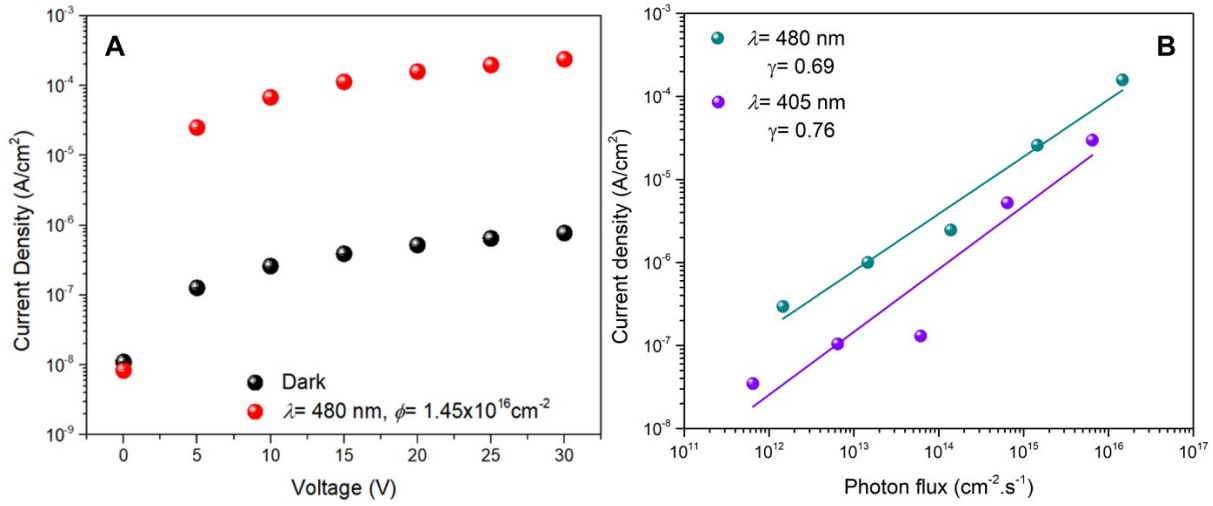

Figure S2– (A) *I-V* curves in the dark and in a condition of high light. (B) Photoresponse curves for the wavelengths of interest for the detection of SA (λ= 405 nm) and AzA (λ= 480 nm). The slope of the fit, γ, is correlated to the generation rate of the sensor.

For the detection of the fluorescent signal in the jasmonic acid assay, it is necessary to block out the excitation light at λ= 405 nm, while maximizing the transmission of the emitted light at λ= 540 nm. To do this, a 1.5 µm thick silicon carbide high-pass filter was deposited on top of the sensor for this assay. The transmission curve of the filter is presented in Figure S3.

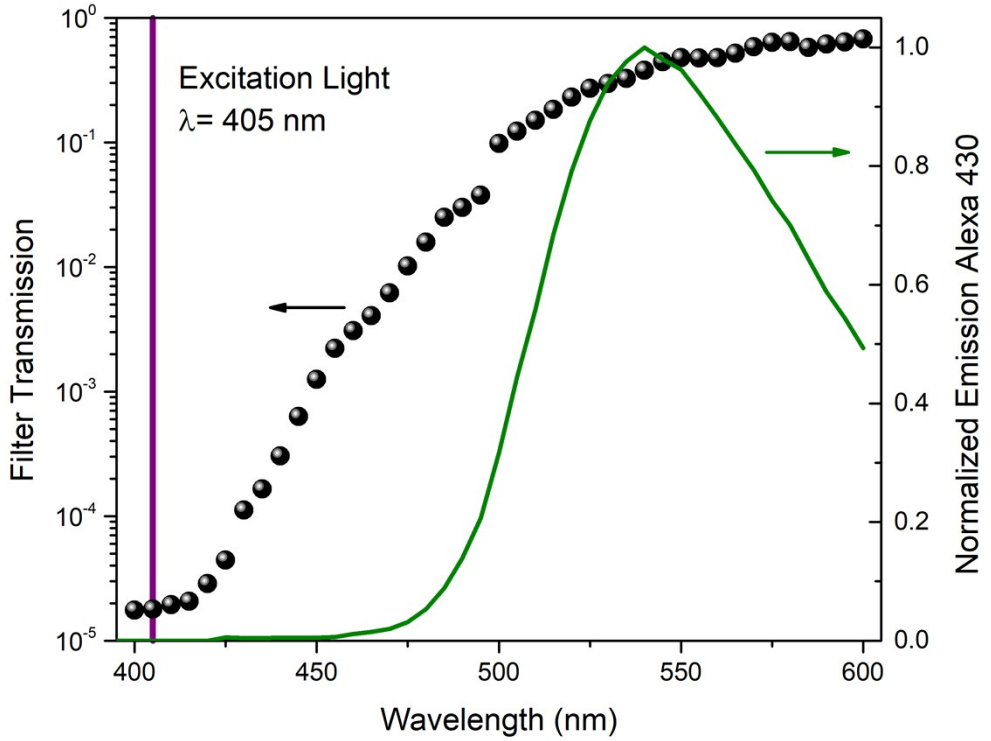

Figure S3 – Overlap of the silicon carbide filter transmission profile (Black dots) with the emission profile of the Alexa 430 ® fluorophore provided by the manufacturer (Green line). The excitation light source used was a λ= 405 nm laser.

To confirm that the a-SiC:H layer did not hinder the performance of the sensor, the photoresponse at *λ*= 540 nm, which is the emission maximum of the Alexa 430® fluorophore, was performed and is presented in Figure S4.

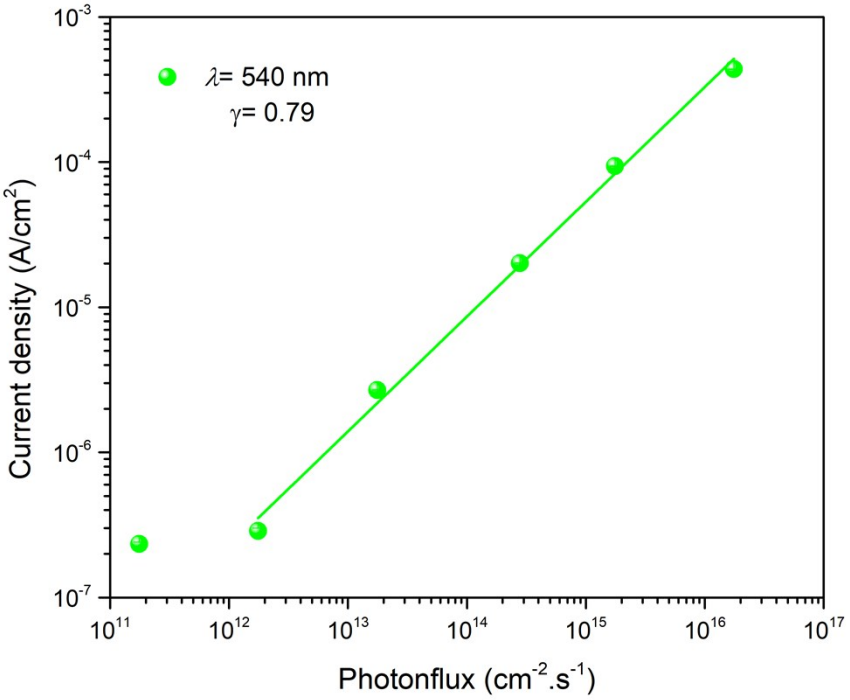

Figure S4 - Photoresponse curve for the wavelength of interest for the detection of JA (λ= 540 nm) using the a-SiC:H-filtered photoconductor. The slope of the fit, γ, is correlated to the generation rate of the sensor

S3 – SA Assay Absorbance Behavior

To determine the optimal wavelength for the detection of SA through the complexation reaction with the TiO_2 nanoparticles, the absorbance spectrum of free SA, free TiO_2 and the product of reaction were measured and are presented in Figure S5.

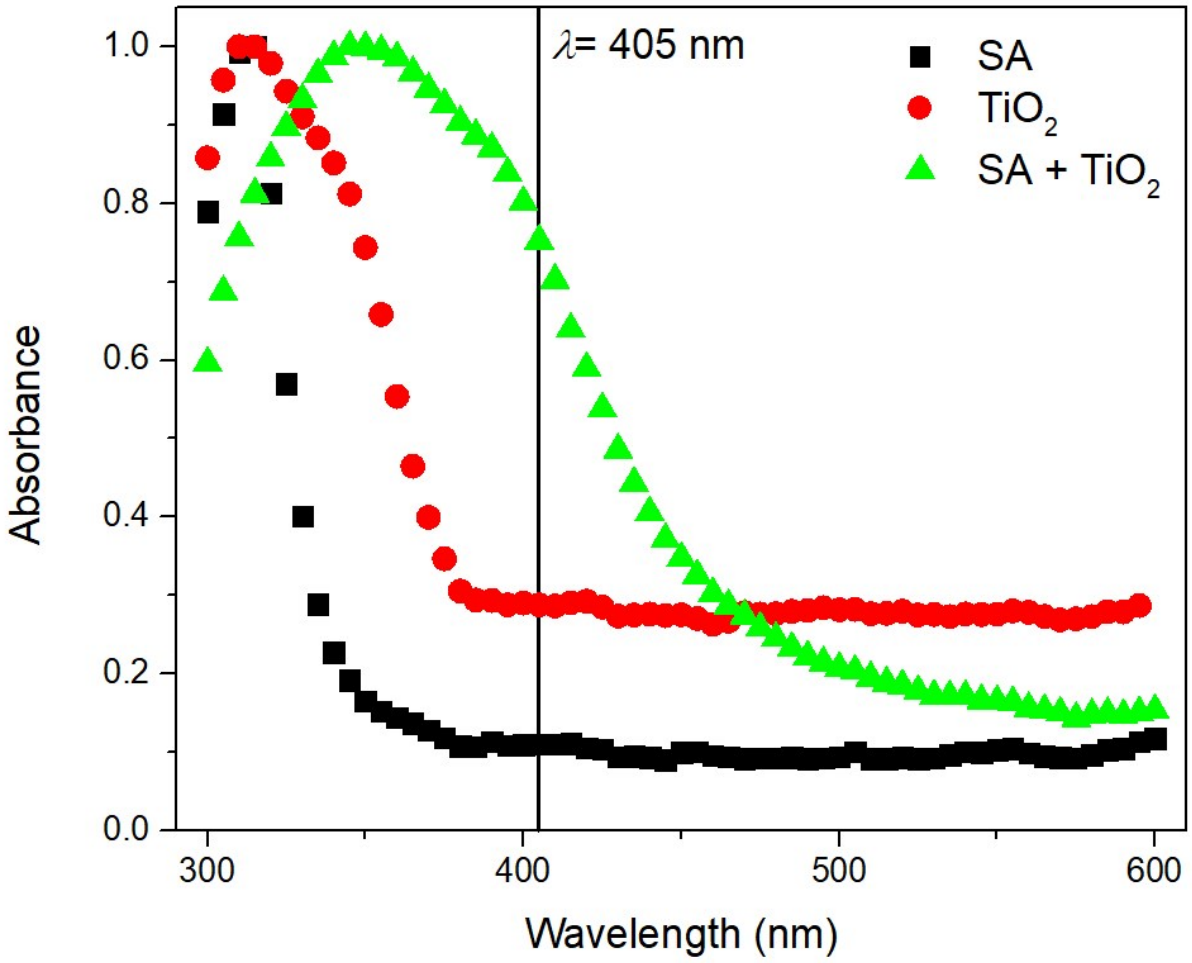

Figure S5 – Absorbance spectra of free SA (black), free TiO2 nanoparticles (red) and the product of the reaction (green). The shift in absorbance from the UV range into the visible due to the reaction is visible here. The vertical line at λ= 405 nm represents the chosen wavelength for the assay.

S4 – TiO_2 Interference assays

Since the assay for the detection of AzA is directly downstream to the chamber for the detection of SA, there is the possibility that the TiO_2 nanoparticles could seep through the first chamber and interfere with the detection of AzA. To determine if any interferences were present, known concentrations of AzA and TiO_2 were mixed together and tested using the AzA enzymatic assay. These results are presented in Figure S6.

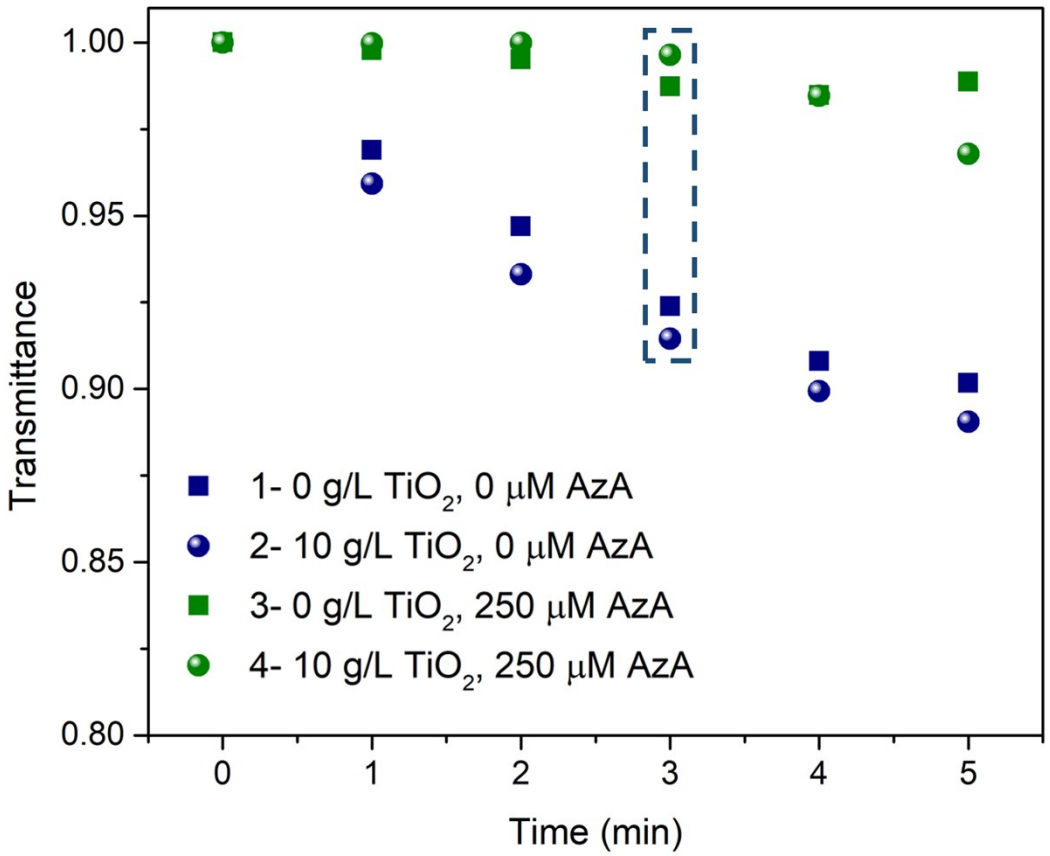

Figure S6 – Assays performed to determine the existence of interference from the TiO_2 nanoparticles on the enzymatic activity of tyrosinase.

By analyzing the results presented in Figure S6, it is possible to determine that there is no interference caused by the TiO_2 nanoparticles on the detection assay for AzA. In Figure S7 the interference caused by the presence of inorganic salts when mixed with the TiO_2 nanoparticles is demonstrated by using phosphate buffer saline (PBS) and compared to the results using DI-water and a SA solution in water.

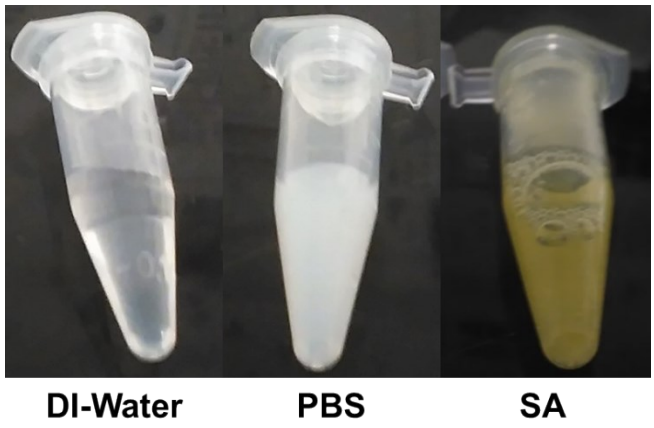

Figure S7 – Result of mixing the TiO_2 nanoparticles with DI-water, PBS and SA. It is important to notice the turbidity caused by the presence of PBS.